IJOER
RESEARCH JOURNAL

International Journal of Engineering Research & Science

ISSN
2395-6992

www.ijoer.com
www.adpublications.org

Volume-7! Issue-3! March, 2021 www.ijoer.com ! info@ijoer.com

Preface

We would like to present, with great pleasure, the inaugural volume-7, Issue-3, March 2021, of a scholarly journal, *International Journal of Engineering Research & Science*. This journal is part of the AD Publications series *in the field of Engineering, Mathematics, Physics, Chemistry and science Research Development*, and is devoted to the gamut of Engineering and Science issues, from theoretical aspects to application-dependent studies and the validation of emerging technologies.

This journal was envisioned and founded to represent the growing needs of Engineering and Science as an emerging and increasingly vital field, now widely recognized as an integral part of scientific and technical investigations. Its mission is to become a voice of the Engineering and Science community, addressing researchers and practitioners in below areas

Chemical Engineering	
Biomolecular Engineering	Materials Engineering
Molecular Engineering	Process Engineering
Corrosion Engineering	
Civil Engineering	
Environmental Engineering	Geotechnical Engineering
Structural Engineering	Mining Engineering
Transport Engineering	Water resources Engineering
Electrical Engineering	
Power System Engineering	Optical Engineering
Mechanical Engineering	
Acoustical Engineering	Manufacturing Engineering
Optomechanical Engineering	Thermal Engineering
Power plant Engineering	Energy Engineering
Sports Engineering	Vehicle Engineering
Software Engineering	
Computer-aided Engineering	Cryptographic Engineering
Teletraffic Engineering	Web Engineering
System Engineering	
Mathematics	
Arithmetic	Algebra
Number theory	Field theory and polynomials
Analysis	Combinatorics
Geometry and topology	Topology
Probability and Statistics	Computational Science
Physical Science	Operational Research
Physics	
Nuclear and particle physics	Atomic, molecular, and optical physics
Condensed matter physics	Astrophysics
Applied Physics	Modern physics
Philosophy	Core theories

Chemistry	
Analytical chemistry	Biochemistry
Inorganic chemistry	Materials chemistry
Neurochemistry	Nuclear chemistry
Organic chemistry	Physical chemistry
Other Engineering Areas	
Aerospace Engineering	Agricultural Engineering
Applied Engineering	Biomedical Engineering
Biological Engineering	Building services Engineering
Energy Engineering	Railway Engineering
Industrial Engineering	Mechatronics Engineering
Management Engineering	Military Engineering
Petroleum Engineering	Nuclear Engineering
Textile Engineering	Nano Engineering
Algorithm and Computational Complexity	Artificial Intelligence
Electronics & Communication Engineering	Image Processing
Information Retrieval	Low Power VLSI Design
Neural Networks	Plastic Engineering

Each article in this issue provides an example of a concrete industrial application or a case study of the presented methodology to amplify the impact of the contribution. We are very thankful to everybody within that community who supported the idea of creating a new Research with IJOER. We are certain that this issue will be followed by many others, reporting new developments in the Engineering and Science field. This issue would not have been possible without the great support of the Reviewer, Editorial Board members and also with our Advisory Board Members, and we would like to express our sincere thanks to all of them. We would also like to express our gratitude to the editorial staff of AD Publications, who supported us at every stage of the project. It is our hope that this fine collection of articles will be a valuable resource for *IJOER* readers and will stimulate further research into the vibrant area of Engineering and Science Research.

Mukesh Arora

(Chief Editor)

Board Members

Dr. Mohamed Abdel Fatah Ashabrawy Moustafa

PhD. in Computer Science - Faculty of Science - Suez Canal University University, 2010, Egypt.

Assistant Professor Computer Science, Prince Sattam bin AbdulAziz University ALkharj, KSA.

Dr. Heba Mahmoud Mohamed Afify

Ph.D degree of philosophy in Biomedical Engineering, Cairo University, Egypt worked as Assistant Professor at MTI University.

Dr. Aurora Angela Pisano

Ph.D. in Civil Engineering, Currently Serving as Associate Professor of Solid and Structural Mechanics (scientific discipline area nationally denoted as ICAR/08"–"Scienza delle Costruzioni"), University Mediterranea of Reggio Calabria, Italy.

Dr. Faizullah Mahar

Associate Professor in Department of Electrical Engineering, Balochistan University Engineering & Technology Khuzdar. He is PhD (Electronic Engineering) from IQRA University, Defense View,Karachi, Pakistan.

Dr. S. Kannadhasan

Ph.D (Smart Antennas), M.E (Communication Systems), M.B.A (Human Resources).

Dr. Christo Ananth

Ph.D. Co-operative Networks, M.E. Applied Electronics, B.E Electronics & Communication Engineering Working as Associate Professor, Lecturer and Faculty Advisor/ Department of Electronics & Communication Engineering in Francis Xavier Engineering College, Tirunelveli.

Dr. S.R.Boselin Prabhu

Ph.D, Wireless Sensor Networks, M.E. Network Engineering, Excellent Professional Achievement Award Winner from Society of Professional Engineers Biography Included in Marquis Who's Who in the World (Academic Year 2015 and 2016). Currently Serving as Assistant Professor in the department of ECE in SVS College of Engineering, Coimbatore.

Dr. Maheshwar Shrestha

Postdoctoral Research Fellow in DEPT. OF ELE ENGG & COMP SCI, SDSU, Brookings, SD Ph.D, M.Sc. in Electrical Engineering from SOUTH DAKOTA STATE UNIVERSITY, Brookings, SD.

Zairi Ismael Rizman

Senior Lecturer, Faculty of Electrical Engineering, Universiti Teknologi MARA (UiTM) (Terengganu) Malaysia Master (Science) in Microelectronics (2005), Universiti Kebangsaan Malaysia (UKM), Malaysia. Bachelor (Hons.) and Diploma in Electrical Engineering (Communication) (2002), UiTM Shah Alam, Malaysia

Dr. D. Amaranatha Reddy

Ph.D.(Postdocteral Fellow,Pusan National University, South Korea), M.Sc., B.Sc. : Physics.

Dr. Dibya Prakash Rai

Post Doctoral Fellow (PDF), M.Sc.,B.Sc., Working as Assistant Professor in Department of Physics in Pachhuncga University College, Mizoram, India.

Dr. Pankaj Kumar Pal

Ph.D R/S, ECE Deptt., IIT-Roorkee.

Dr. P. Thangam

BE(Computer Hardware & Software), ME(CSE), PhD in Information & Communication Engineering, currently serving as Associate Professor in the Department of Computer Science and Engineering of Coimbatore Institute of Engineering and Technology.

Dr. Pradeep K. Sharma

PhD., M.Phil, M.Sc, B.Sc, in Physics, MBA in System Management, Presently working as Provost and Associate Professor & Head of Department for Physics in University of Engineering & Management, Jaipur.

Dr. R. Devi Priya

Ph.D (CSE),Anna University Chennai in 2013, M.E, B.E (CSE) from Kongu Engineering College, currently working in the Department of Computer Science and Engineering in Kongu Engineering College, Tamil Nadu, India.

Dr. Sandeep

Post-doctoral fellow, Principal Investigator, Young Scientist Scheme Project (DST-SERB), Department of Physics, Mizoram University, Aizawl Mizoram, India- 796001.

Mr. Abilash

MTech in VLSI, BTech in Electronics & Telecommunication engineering through A.M.I.E.T.E from Central Electronics Engineering Research Institute (C.E.E.R.I) Pilani, Industrial Electronics from ATI-EPI Hyderabad, IEEE course in Mechatronics, CSHAM from Birla Institute Of Professional Studies.

Mr. Varun Shukla

M.Tech in ECE from RGPV (Awarded with silver Medal By President of India), Assistant Professor, Dept. of ECE, PSIT, Kanpur.

Mr. Shrikant Harle

Presently working as a Assistant Professor in Civil Engineering field of Prof. Ram Meghe College of Engineering and Management, Amravati. He was Senior Design Engineer (Larsen & Toubro Limited, India).

Table of Contents

Volume-7, Issue-3, March 2021

Energy Savings in Renewable Integrated Distribution Network and Impact of Storage Devices

Bharat Singh[1*], Jagnadan Negi[2], Satyaveer Singh Rawat[3]

Electrical Engineering Department, NIT Kurukshetra, Haryana, India
*Corresponding Author:
Bharat Singh, Ph.D. Scholar, Electrical Engineering Department, NIT Kurukshetra, Haryana, India

Received: 28 February 2021/ Revised: 7 March 2021/ Accepted: 13 March 2021/ Published: 31-03-2021

***Abstract*—** *Energy loss reduction is a significant issue for Renewable energy planning in the Distribution system. The high penetration of wind and solar became the primary task for the optimal size of energy storage to support the power mismatch. In the present work, energy savings have been obtained in a renewable integrated distribution system. The impact of the energy storage device has also been evaluated. The main contribution of this paper is:*

(i) Optimal location of DGs and battery are obtained by solving single and multi-objective functions.

(ii) Determination of DG and battery size for loss savings.

(iii) Impact of battery energy storage device on loss profile and total cost of the system.

The simulation results of the test system have been compared with other existing results.

***Keywords*— Radial distribution system, Battery energy storage device, Energy Loss minimisation, optimal sizing and siting, Renewable Energy sources.**

I. INTRODUCTION

The intermittent behaviour of renewable energy generation has become an essential issue for power deficiency in the distribution network. Therefore, the optimal economical operation for storage devices has to be analysed for supporting power mismatch. The losses along the distribution system are much higher with a higher value of R/X component of the line as compares to the transmission system. Therefore, the loss minimization in distribution system has become an essential issue. Many of the utilities have been used to compensate for the loss in the distribution network. Therefore, the location and sizing of DGs is the major issue in the distribution network. The co-ordination of energy saving with the overall cost of the system is another issue in the system.

A lot of literature is available for optimal placement of DGs to minimize the power loss and voltage deviations in a network. Authors in [1] presented the annual energy loss minimization with the integration of DGs in the network. The optimal DG placement using Stud Krill herd Algorithm (SKHA) for the radial distribution system in [2]. The population-based Gbest-guided Artificial Bee Colony (GABC) optimization algorithm has used to minimize the power loss and determine the impact of shunt capacitor with DG placement [3]. Many of the literature is based on the nature-inspired algorithm. In this way, the optimal location of DG has been obtained by using Dragonfly algorithm [4]. An improved particle swarm optimization has been used for the installation of DG in Microgrid (MG) system [5]. The analytical representations are used to obtain the size of DG at various locations for total loss minimisation. The loss saving equations was also represented in [6]. The different types of voltage-dependent loads and a separate line XR ratios have taken into account to study the distribution load flow [7]. Murty et al. [8] have considered the multi-objective based optimization problem for the uncertainty nature of renewable power generation. The reactive power support has also been done using the installation of DG location in [9]. The optimal power factor has considered for the position of DG to minimize the power loss using PSO algorithm by Kansal et al. [10]. The Mixed Integer Non-Linear Programming (MINLP) formulation has introduced in [11] for loss minimization. The DG location has been obtained by combined power loss sensitivity (CPLS) approach; however, the battery storage was not considered. The clearness index of probability density function (pdf) has been used along with Monte Carlo simulation (MCS) to model the solar irradiance [12]; however, the battery energy support has not considered. MG with four different types of DG has obtained to minimize power loss and to regulate the bus voltage also. In the literature [1-11] the power loss scenario-based optimal location of DGs was obtained. Yet, battery storage has not been found in the literature [1-11].

The combined dispatch strategy for battery along with PV-Diesel system has been implemented in the HOGA (Hybrid Optimisation by Genetic Algorithms) program [13]. The wind-based Distribution generation (DG) has not considered. The multi-source based hybrid generation with battery storage using PSO algorithm has been taken into account to minimize the total power loss [14]. The battery size determination has reviewed in [15] with various indicators likewise, financial, technical and hybrid indicators. (i) In the Financial index, the local currency has become the decision making for the benefit and overall cost of the battery in renewable energy sources (RES). The net present value (NPV) of the battery energy storage system (BESS) [16] has represented to achieve the sizing and placement of ESS. An optimal scheduling analysis for the vanadium redox battery (VRB) has described based on cost-benefit review for MG application [17]. In the technical index, the ESS has to support the dynamic and steady-state behaviour of RES in the MG system. The risk-informed decision-making process has introduced to obtain the size of battery storage by using the probabilistic approach [18]. In the composite index, the battery size has been obtained by considering both financial and technical indicators. The size of battery storage has been determined by considering the electricity market for the wind power plant [19]. The battery storage has also been emphasized the operation and economics of the wind power intermittency. The analysis has been carried out to obtain the daily energy savings with DGs and the impact of battery energy device on the savings.

II. PROBLEM FORMULATION AND MATHEMATICAL MODEL

The main objective of the paper is; to obtain optimal location and size of DG along with battery storage devices for minimization of the Daily energy loss of the network. The single and multi objectives have been considered for the analysis.

The single objective problem has formulated as:

- **Minimize the Daily energy loss with DGs and battery storage devices.**

The problem has been solved in two parts.

In the first part: (i): The location of DGs has obtained determining the Daily energy loss minimization using PSO (Particle Swarm Optimization) algorithm. The location of battery storage has been obtained using the combined dispatch strategy in the PSO algorithm.

In the second part: (ii): The size of DGs and battery storage was obtained solving the problem with the MINLP (Mixed Integer Non-Linear Programming) in GAMS.

The multi-objective problem was formulated as:

- **Minimisation of the cost of Daily energy loss and the total cost of the system**

The total cost of the system consists of the cost of energy loss (CEL), the fuel cost of diesel generator, operation and maintenance cost, replacement cost, and initial installation cost of DG, PV, battery, regulator, invertors etc.

2.1 Mathematical Model and formulation

2.1.1 Single objective function

- **Minimization of Daily energy loss as:**

$$OF1 = \sum_{k=1}^{T} \left(\sum_{j=1}^{nl} PL_{ij} \right) \cdot \Delta k \tag{1}$$

Where, PL_{ij} is the total active power loss in the line respectively? Δk is the time duration in hrs.

2.1.2 Multi-objective function

- **Minimization of cost of energy loss and the cost of the DGs as:**

$$OF2 = min\left\{ C_e.TE_{Loss}^{i} + \sum_{k=1}^{T} NPV_{Batt} + \sum_{k=1}^{T} \left(NPV_{DG}^{Ren} + NPV_{DG}^{Diesel} \right) \right\} \tag{2}$$

Where,

$$TE_{Loss}^{i} = 365 \times \sum_{k=1}^{T}\left(\sum_{j=1}^{nl} PL_{ij}\right) \cdot k$$

$$NPV_{Batt} = \sum_{i=1}^{nb}(N_{inv}(i) \cdot NPV_{inv} + N_{batt}(i) \cdot NPV_{batt})$$

$$NPV_{DG}^{Diesel} = Pr_{fuel} \cdot \left(\sum_{i}^{nb} fuel_{consumed}\right) \cdot T$$

$$NPV_{DG}^{Ren} = \sum_{i}^{nb}(N_{PV}(i) \cdot NPV_{PV} + N_{wind}(i) \cdot NPV_{wind} + N_{reg}(i) \cdot NPV_{reg} \quad (3)$$

The net present values for all components are given as:

$$NPV = Cost_{Aqu} + Cost_{O\&M} + Cost_{Rep} \quad (4)$$

$Cost_{Aqu}$, is the acquisition cost, C_e is cost of the energy loss,$Cost_{O\&M}$ is the operation and maintenance cost, $Cost_{Rep}$ is the replacement cost. N_{PV}, N_{wind} , N_{batt}, N_{reg}, N_{inv} is the number of PV panel, wind turbine, battery, regulator, invertors respectively. NPV_{PV}, NPV_{wind}, NPV_{batt}, NPV_{reg}, NPV_{inv} is the net present value for PV, wind , battery, regulator, and inverter respectively. $fuel_{consumed}$ is fuel consumed by the DEGs, Pr_{fuel} is the fuel price (litter/kWh), and T is the total time period of operation.

2.1.3 The equality and inequality constraints are:

- **The power balance equations are:**

$$P_i^k = \left(Pg_i^k - Pd_i^k\right) = V_i^k \sum_{j=1}^{n} V_j^k \left(G_{ij}^k \cos\left(\delta_i^k - \delta_j^k\right) + B_{ij}^k \sin\left(\delta_i^k - \delta_j^k\right)\right) \quad (5)$$

$$Q_i^k = \left(Qg_i^k - Qd_i^k\right) = V_i^k \sum_{j=1}^{n} V_j^k \left(G_{ij}^k \sin\left(\delta_i^k - \delta_j^k\right) - B_{ij}^k \cos\left(\delta_i^k - \delta_j^k\right)\right) \quad (6)$$

$$\forall\, i \in S_B \,\&\, k \in S_T$$

where $\forall i = 1,2 \ldots .\, nb$, $\forall j = 1,2 \ldots .\, nl$, nb is a number of buses and nl is the total number of line. S_B is the set of buses, and S_T is the set of Time k. Pd_i^k and Qd_i^k are the active and reactive power demand for i^th^ bus at k^th^ time period.

- **Power generation constraints:**

$$Pg_i^k = P_{deg}{}_i^k + N_{wind}(i) \cdot P_{wind}{}_i^k + N_{PV}(i) \cdot P_{PV}{}_i^k + N_{batt}(i) \cdot \left(P_{ch}{}_i^k - P_{dis}{}_i^k\right) \quad (7)$$

$$Qg_i^k = Q_{deg}{}_i^k + N_{wind}(i) \cdot Q_{wind}{}_i^k \quad (8)$$

Where, $P_{deg}{}_i^k$ and $Q_{deg}{}_i^k$ are the active and reactive power supplied by diesel generator for i^{th} bus at k^{th} time period.

2.1.4 Power Loss equation

$$\left|P_{ij}^k\right| = \left|V_i^k V_j^k \left(G_{ij}^k \cos\left(\delta_i^k - \delta_i^k\right) + B_{ij}^k \cos\left(\delta_i^k - \delta_i^k\right)\right) - (V_i^k)^2 G_{ij}^k\right| \le Pl_{max}^k \quad (9)$$

Where, Pl_{max}^k is the maximum apperent power flow through the line at kth hrs. $l \in S_L$is the set of line.

Inequality constraints:

2.1.5 Constraints for Transmission line

$$P_{fsmin}{}_j^k \le P_{fs}{}_j \le P_{fsmax}{}_j^k,\ i \in S_{fs}$$

$$Q_{fsmin}{}_i^k \le Q_{fs}{}_j \le Q_{fsmax}{}_j^k,\ i \in fs \text{ r}$$

$$P_{frmin}{}_j^k \le P_{fr}{}_j \le P_{frmax}{}_j^k,\ i \in S_{fr}$$

$$Q_{frmin}{}_i^k \le Q_{fr}{}_j \le Q_{frmax}{}_j^k,\ i \in S_{fr} \quad (10)$$

2.1.6 Capacity Limits of the distribution generation system

$$P_{Gi}^{min} \le Pg_i \le P_{gi}^{max},\ i \in S_G \quad (11)$$

$$Q_{gi}^{min} \le Qg_i \le Q_{gi}^{max},\ i \in S_G \quad (12)$$

2.1.7 Voltage and angle limits

$$V_i^{min} \leq V_i \leq V_i^{max}, \ i \in S_B \tag{13}$$

$$\delta_{min}{}_j^k \leq \delta_i \leq \delta_{max}{}_j^k, \ \forall i = 1,2 \ldots .nb \tag{14}$$

2.1.8 Power factor limits

$$pf_i^{lo} \leq pf_i \leq pf_i^{up}, \ i \in S_B \tag{15}$$

2.2 Mathematical modelling of energy sources

In this section, the mathematical modelling of renewable-based DGs, diesel generator based DG and battery energy storage is given.

2.2.1 Modelling of wind power generation

The quadratic model of wind power generation has been taken for analysis. The wind turbine model is as:

$$P_{wind} = \begin{cases} P_{rated} \cdot \left({(v_{rated} - v_{in})^2} \big/ {(v_r - v_{in})^2} \right); & v_{in} \leq v_{rated} \leq v_r \\ P_{rated}; & v_r \leq v_{rated} \leq v_{out} \\ 0 \quad ; & v_{rated} > v_{out} \ and \ v_{rated} < v_{cut} \end{cases} \tag{16}$$

Where, P_{wind} is the wind power output, P_{rated} is the rated wind power, v_{in} is cut in the velocity of wind, v_{out} is cut out wind velocity. The Fig.1 shows the wind turbine output vs wind velocity curve. The cut in the velocity of the wind v_{in} is 3 (m/s), cut outv_{out} is 20 (m/s) and rated velocity v_{rated} is 13 (m/s) carried out for analysis.

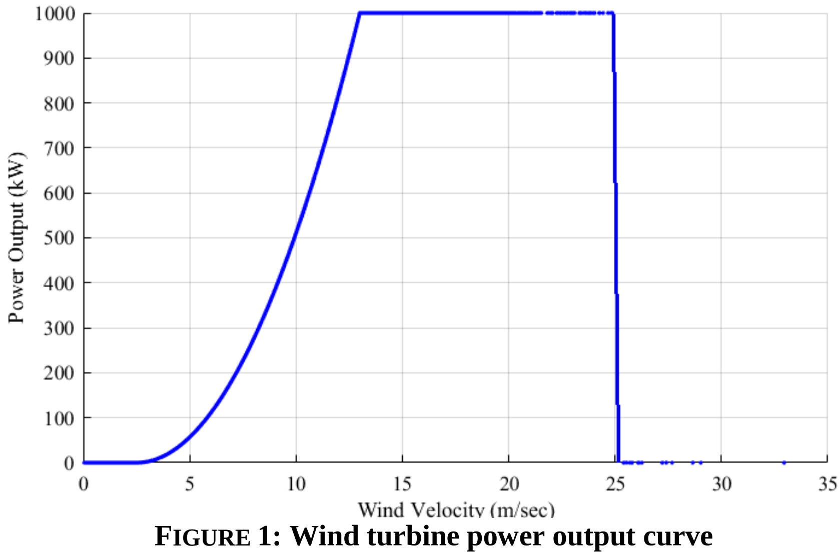

FIGURE 1: Wind turbine power output curve

2.2.2 Modelling of PV- based DG

The renewable source of energy, PV generator provides the DC current at 48 V. The PV generator output has been obtained using the Monte Carlo Simulation (MCS).

The solar PV model is:

$$P_{solar}\left(I_\beta\right) = N_{PV} \cdot FF \cdot V \cdot I \tag{17}$$

where, 1000 number of samples are taken for MCS,P_{solar} is the output power, FF is the fillfactor, V is the rated DC voltage, I is the DC current output, and N_{PV} is the total number of solar panel [12]. The PV generator power output over 24 hrs is shown in Fig.2.

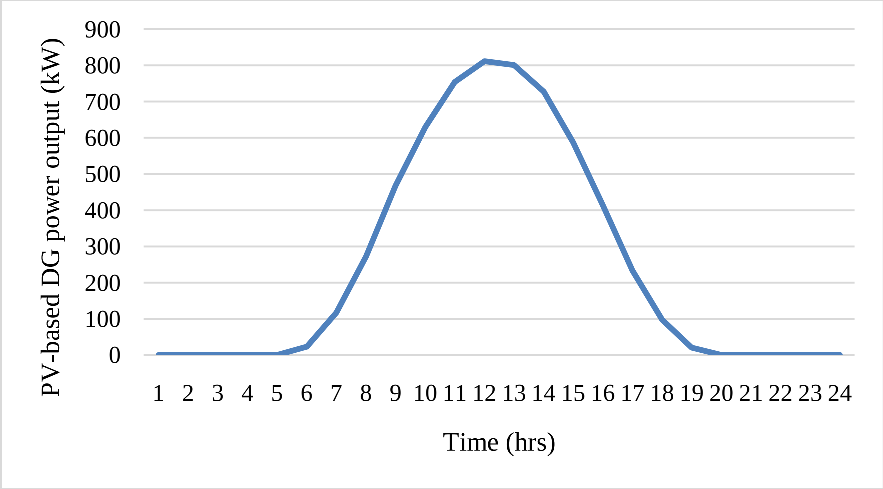

FIGURE 2: Solar power output curve for 24 hrs

2.2.3 Diesel generator

The diesel generator-based DG has been considered to backup for system power requirement. The diesel generator can charge the battery and supply the load demand for a short period according to the dispatch strategy. The linear model of fuel consumption for diesel generator has been considered for analysis [13]. The fuel consumption can be represented as:

$$fuel_{consumed} = B_{fuel} \cdot P_{NGen} + A_{fuel} \cdot P_{Gen} \cdot \frac{1}{h} \quad (18)$$

where, P_{NGen} is Diesel Generator (DEG) rated power in kW, P_{Gen} is the output power A and B are the fuel curve coefficient. The value of A_{fuel} is 0.246 $\left(\frac{l}{kWh}\right)$ and B_{fuel} is 0.08415[14].

2.2.4 Radial Distribution system

The radial distribution system network of 100 kVA, 12.66 kV, IEEE 33-buss system has considered as a test system. The radial distribution system has 33 buses and 32 branches [7].

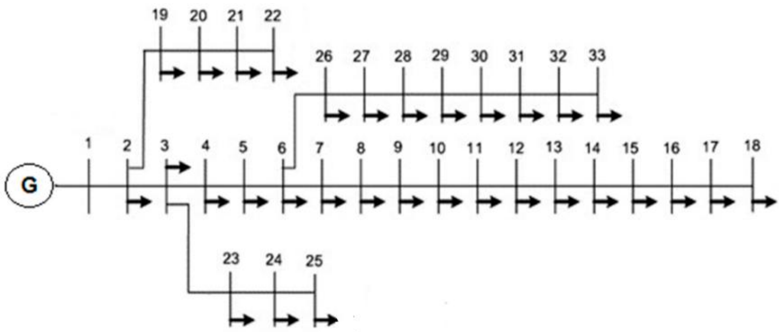

FIGURE 3: Equivalent circuit model of Radial Distribution system

Thesingle line diagram of IEEE 33 bus radial distribution system is shown inFig.3.

III. ALGORITHM

In this section, the various steps have explained to solve the optimization problem using MINLP solver in GAMS. The MATLAB and GAMS interfacing has also been described in this algorithm for solving the hybrid optimization algorithm.

3.1 The hybrid PSO and GAMS algorithm

In the proposed hybrid optimization algorithm from step 1 to 4; the PSO algorithm has used. Whereas in step 5 to step 8, the MINLP solver in GAMS has used for obtaining the size of DGs and battery storage.

Step 1:

(a) Initialize the random population for PSO algorithm.
(b) Solve the equation for wind and solar power calculation

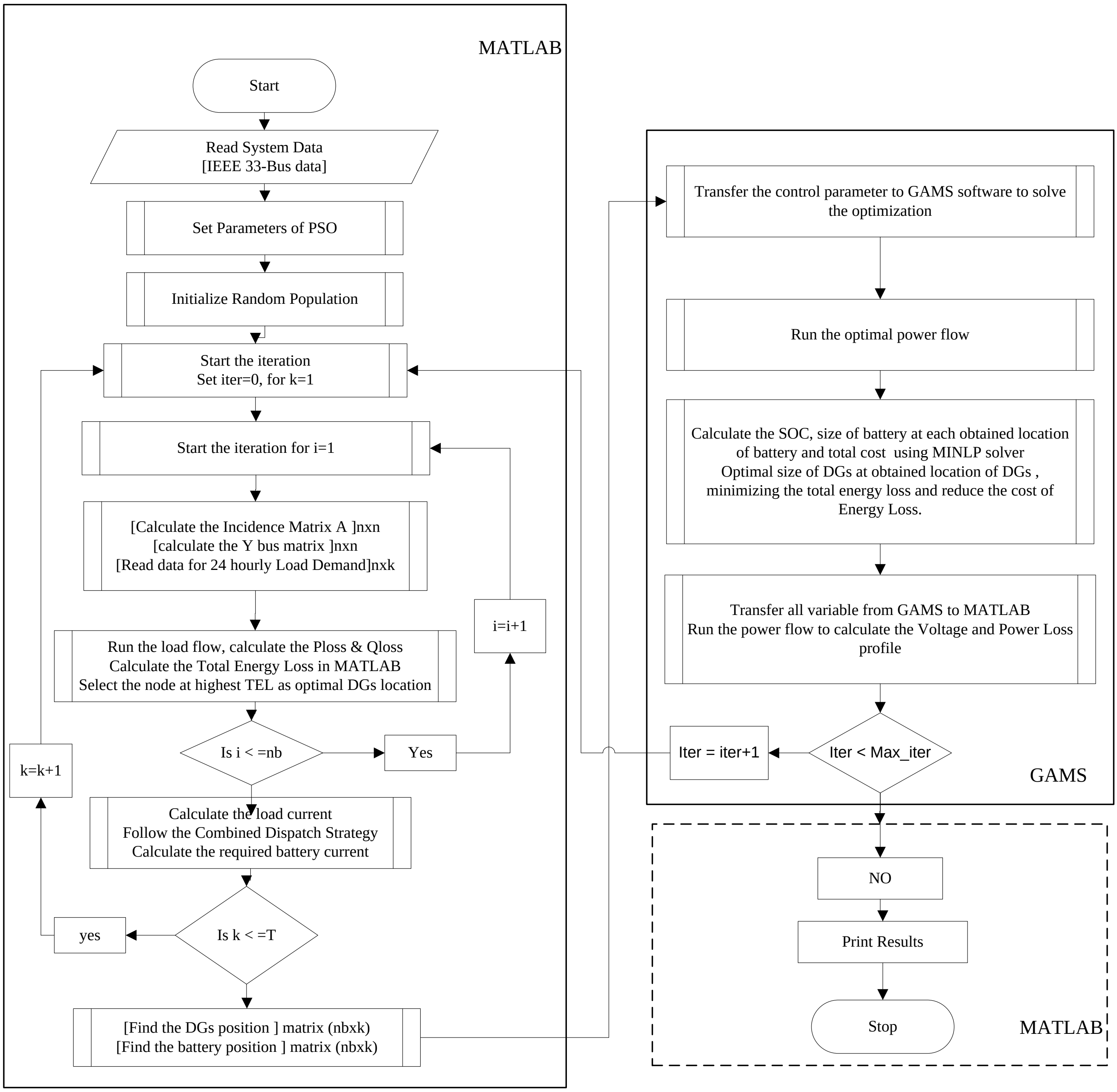

FIGURE 4: Flow chart for hybrid GAMS and PSO optimization

Step 2:

(a) Run the load flow program for 24-hrs and obtain the base Case Daily energy loss using PSO algorithm.

(b) Select the candidate node having the highest energy loss for DG location. Save the place for DGs.

Step 3: Solve the combined dispatch strategy for each buses i=1to nb and k=1 to 24 hrs.

(a) Obtain the position of batteries at each node determining the net load current from step 2(a).

(b) The iteration for i^{th} bus and k^{th} time solve up to $i \leftarrow i+1; k \leftarrow k+1$. If $i < nb$ and k$< T$; go for step 2 otherwise go to next step.

Step 4: After obtaining the location of the candidate node, the size of DGs, along with battery storage, has determined. Transfer the all control parameter from MATLAB to GAMS.

(a) Solve the objective function.

(b) Obtain the size of the battery, SOC, charging and discharging of the cell.

(c) Obtain the size of DG.

Step 5: Transfer the objective variables form GAMS to MATLAB.

(a) Get the results

Step 6: Print the results.

The flow chart of the proposed hybrid algorithm is shown in Fig.4.

IV. RESULTS AND DISCUSSIONS

The results are obtained for the IEEE 33 bus radial distribution system having DGs along with the storage devices.

In objective (i) two Cases have been considered as;

- Base Case: Without DGs and Battery storage devices.
- Case 1: Single DG with Battery Storage Devices.
- Case 2: Two DGs with Battery Storage Devices.

4.1 Results for Single Objective Function

The results are obtained for IEEE-33 bus test system. The total demand for the test system is $3715 + j2300$ kVA.

4.1.1 Results for Base Case

The load data is shown in Fig.5. The Daily energy demand for 24 hrs load variation is 73.9285 MWh. The minimum voltage found is 0.9037 pu at bus number 18. The Daily energy loss for a day obtained is 2031.45 kWh. The annual cost of energy loss (CEL) obtained is 88,712.8 (€).The results are also compared with the base Case and other existing methods and techniques.

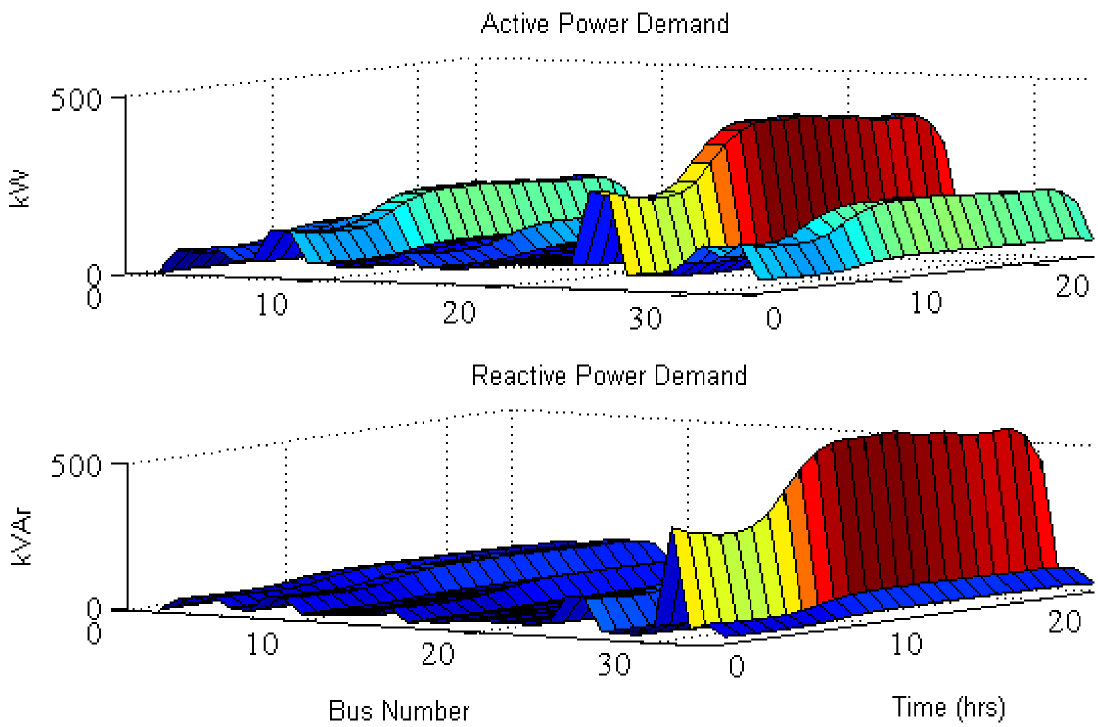

FIGURE 5: Load Demand for 24 hrs.

4.1.2 Case 1: Result for Single DG

The Daily energy loss profile for single DG without battery storage device is shown in Fig.6.

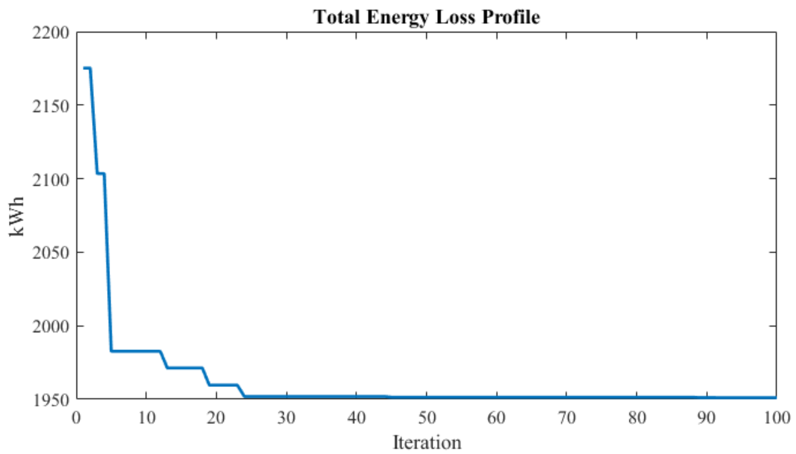

FIGURE 6: Daily energy Loss Profile for single- DG with PSO algorithm

The Daily energy loss obtained without battery storage is 1950 kWh for 24 hrs load variation. The daily energy loss profile without battery is shown in Fig. 6.

The daily energy loss obtained with battery storage and single DG is 1062.2 kWh for 24 hrs load variation. The size and location of DGs along with battery storage is shown in Fig. 7. The size of single DG obtained is 1355.7 kW at bus number 6^{th}. The maximum size of battery obtained is 116.736 kWh at bus number 26^{th}. The optimal location of battery storage is selected using combined dispatch strategy. The maximum and minimum numbers of battery cell obtained are 8 and 4, respectively.

In this scenario, the Daily energy loss has been reduced from the of 1950 kWh to 1062.2 kWh with using both the DGs and the battery energy storage. The percentage of energy loss reduction obtained using the DG with battery storage is 45.52% compared with the single DG only.

4.1.3 Case 2: Result for Two DGs.

The Daily energy loss profile for two DGs without battery storage device is shown in Fig.7. The energy loss has been reduced from 2150 kWh to 1750.56 kWh by using DG without battery storage. The PSO algorithm is conversed up to 50 iterations beyond it the energy loss curve is flat.

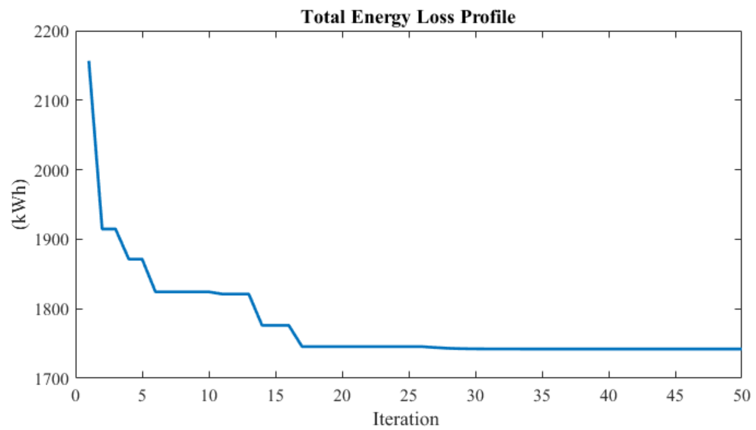

FIGURE 7: Daily energy Loss Profile for Two DGs with PSO algorithm

The size of renewable-based DGs obtained are 655.74, 901.6394 at 13^{th} and 30^{th} bus respectively. The total size of diesel generator obtained is 120 kW and the maximum size of battery storage is 58.368 kWh at 26^{th} bus.

The energy loss has been reduced from base case of 2031.5 kWh to 821.84 kWh by using battery energy storage and DGs. The percentage of energy loss reduction obtained is 59.547% with the base Case.

The daily energy loss obtained is 1750.56 kWh using two DGs only, whereas daily energy loss obtained is 821.84 kWh using two DGs and battery storage. Therefore the percentage of energy loss reduction obtained is 45.528% compared with two DGs without battery storage.

4.2 Voltage Profile and Power Loss

The proposed algorithm has been used to obtain the voltage regulation also. The minimum voltage of Case 1 and Case 2 for 24 hrs load variation is shown in Fig.8.The minimum voltage obtained is 0.9635 pu across 18th bus at 12th hours for Case-1. The minimum voltage obtained is 0.9766 pu across 33rd bus at12th hrs for Case-2.

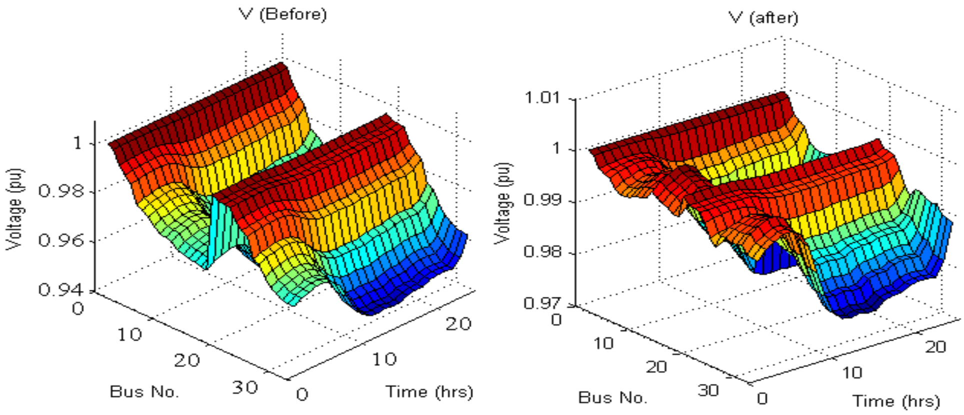

FIGURE 8: Voltage profile for 24 hrs load variation for IEEE 33-bus system

In Fig.9, the minimum voltage profile for 33 bus systems is considered for 24 hrs load variation. The voltage profile has enhanced for Case-2 and Case-1 as compare with the base Case.

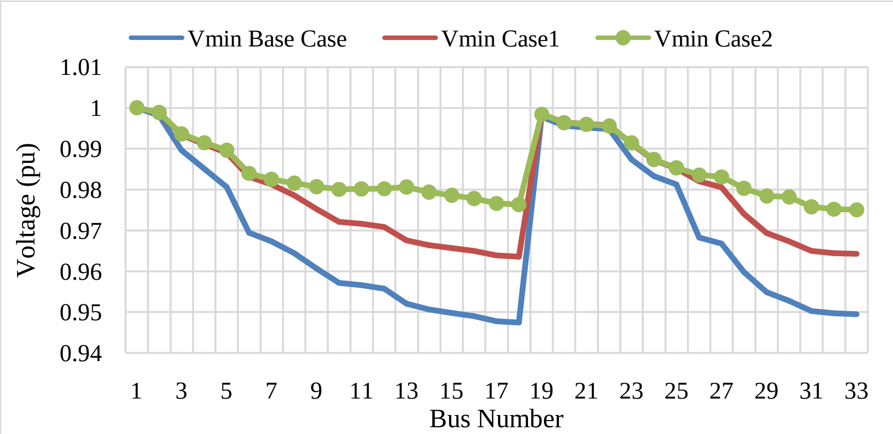

FIGURE 9: Minimum voltage profile for various case studies

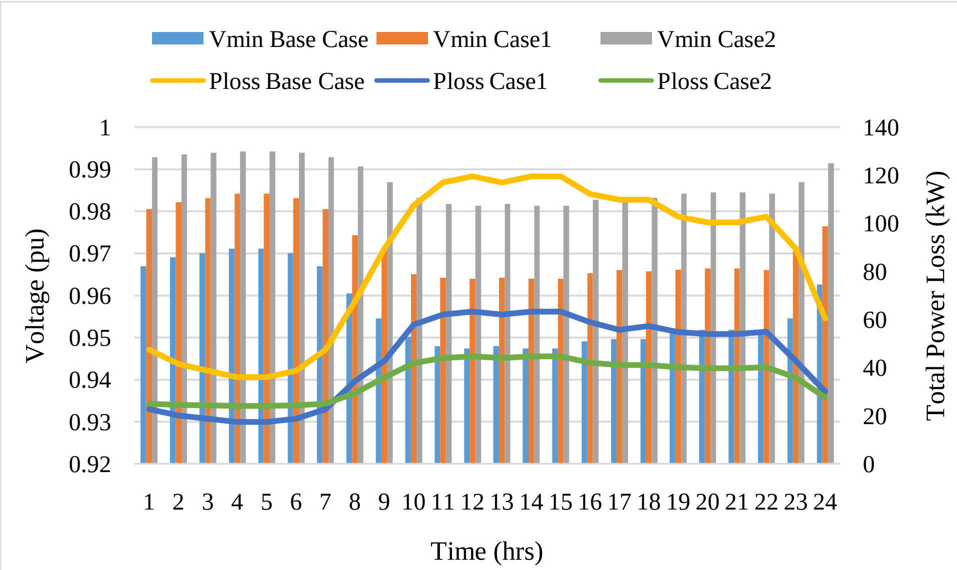

FIGURE 10: The Power loss and voltage profile for 24 hrs load variation

The total power loss and improved voltage profile have been shown in Fig.10 for 24 hrs load variation. The highest voltage at 5^{th} hrs and lowest at 12^{th} hrs have been obtained for each Case. The total power loss has been reduced by increasing the numbers of DGs. Therefore, in Case2; the total power loss and voltage profile have superior results with other Cases. The minimum power loss has obtained with Case-2 at 4^{th} hrs, whereas the highest power loss obtained at 15^{th} hrs.

V. CONCLUSION

This paper represents the hybrid PSO and GAMS optimization using MATLAB and GAMS interfacing to solve the multi-objective problem. This study provides the optimal sizing and siting of battery storage with the integration of renewable sources to minimize the Daily energy loss and cost of the system also. The proposed hybrid algorithm has solved in two parts. (i) In the first part, the PSO algorithm, along with a combined dispatch strategy, has been addressed to obtain the location of DGs and battery storage. (ii) The MINLP algorithm in GAMS has been solved to get the size of DGs and battery storage.

The best combination for economical operation and loss minimization obtained is PV-based, wind-based, diesel-based DG + battery storage.

REFERENCES

[1] D. Q. Hung, N. Mithulananthan, and K. Y. Lee, "Optimal placement of dispatchable and nondispatchable renewable DG units in distribution networks for minimizing energy loss," *Int. J. Electr. Power Energy Syst.*, vol. 55, pp. 179–186, 2014, doi: 10.1016/j.ijepes.2013.09.007.

[2] S. A. ChithraDevi, L. Lakshminarasimman, and R. Balamurugan, "Stud Krill herd Algorithm for multiple DG placement and sizing in a radial distribution system," *Engineering Science and Technology, an International Journal*, vol. 20, no. 2. pp. 748–759, 2017, doi: 10.1016/j.jestch.2016.11.009.

[3] M. Dixit, P. Kundu, and H. R. Jariwala, "Incorporation of distributed generation and shunt capacitor in radial distribution system for techno-economic benefits," *Engineering Science and Technology, an International Journal*, vol. 20, no. 2. pp. 482–493, 2017, doi: 10.1016/j.jestch.2017.01.003.

[4] M. C. V. Suresh and E. J. Belwin, "Optimal DG placement for benefit maximization in distribution networks by using Dragonfly algorithm," *Renewables Wind. Water, Sol.*, vol. 5, no. 1, 2018, doi: 10.1186/s40807-018-0050-7.

[5] S. Xie, X. Wang, C. Qu, X. Wang, and J. Guo, "Impacts of different wind speed simulation methods on conditional reliability indices," *Int. Trans. Electr. energy Syst.*, vol. 20, no. May 2010, pp. 1–6, 2013, doi: 10.1002/etep.

[6] R. Viral and D. K. Khatod, "An analytical approach for sizing and siting of DGs in balanced radial distribution networks for loss minimization," *International Journal of Electrical Power and Energy Systems*, vol. 67. pp. 191–201, 2015, doi: 10.1016/j.ijepes.2014.11.017.

[7] E. Bompard, E. Carpaneto, G. Chicco, and R. Napoli, "Convergence of the backward/forward sweep method for the load-flow analysis of radial distribution systems," *Int. J. Electr. Power Energy Syst.*, vol. 22, no. 7, pp. 521–530, 2000, doi: 10.1016/s0142-0615(00)00009-0.

[8] V. V. V. S. N. Murty and A. Kumar, "Optimal DG integration and network reconfiguration in microgrid system with realistic time varying load model using hybrid optimisation," *IET Smart Grid*, vol. 2, no. 2, pp. 192–202, 2019, doi: 10.1049/iet-stg.2018.0146.

[9] P. Mehta, P. Bhatt, and V. Pandya, "Optimal selection of distributed generating units and its placement for voltage stability enhancement and energy loss minimization," *Ain Shams Eng. J.*, vol. 9, no. 2, pp. 187–201, 2018, doi: 10.1016/j.asej.2015.10.009.

[10] S. Kansal, V. Kumar, and B. Tyagi, "Optimal placement of different type of DG sources in distribution networks," *Int. J. Electr. Power Energy Syst.*, vol. 53, no. 1, pp. 752–760, 2013, doi: 10.1016/j.ijepes.2013.05.040.

[11] S. Kaur, G. Kumbhar, and J. Sharma, "A MINLP technique for optimal placement of multiple DG units in distribution systems," *Int. J. Electr. Power Energy Syst.*, vol. 63, pp. 609–617, 2014, doi: 10.1016/j.ijepes.2014.06.023.

[12] Y. M. Atwa, E. F. El-Saadany, M. M. A. Salama, R. Seethapathy, M. Assam, and S. Conti, "Adequacy evaluation of distribution system including wind/solar DG during different modes of operation," *IEEE Trans. Power Syst.*, vol. 26, no. 4, pp. 1945–1952, 2011, doi: 10.1109/TPWRS.2011.2112783.

[13] R. Dufo-López and J. L. Bernal-Agustín, "Design and control strategies of PV-diesel systems using genetic algorithms," *Sol. Energy*, vol. 79, no. 1, pp. 33–46, 2005, doi: 10.1016/j.solener.2004.10.004.

[14] D. Suchitra, R. Jegatheesan, and T. J. Deepika, "Optimal design of hybrid power generation system and its integration in the distribution network," *Int. J. Electr. Power Energy Syst.*, vol. 82, pp. 136–149, 2016, doi: 10.1016/j.ijepes.2016.03.005.

[15] Y. Yang, S. Bremner, C. Menictas, and M. Kay, "Battery energy storage system size determination in renewable energy systems: A review," *Renew. Sustain. Energy Rev.*, vol. 91, no. June 2017, pp. 109–125, 2018, doi: 10.1016/j.rser.2018.03.047.

[16] C. Chen, S. Duan, T. Cai, B. Liu, and G. Hu, "Optimal allocation and economic analysis of energy storage system in microgrids," *IEEE Trans. Power Electron.*, vol. 26, no. 10, pp. 2762–2773, 2011, doi: 10.1109/TPEL.2011.2116808.

[17] T. A. Nguyen, M. L. Crow, and A. C. Elmore, "Optimal sizing of a vanadium redox battery system for microgrid systems," *IEEE Trans. Sustain. Energy*, vol. 6, no. 3, pp. 729–737, 2015, doi: 10.1109/TSTE.2015.2404780.

[18] M. Yue and X. Wang, "Grid Inertial Response-Based Probabilistic Determination of Energy Storage System Capacity Under High Solar Penetration," *IEEE Trans. Sustain. Energy*, vol. 6, no. 3, pp. 1039–1049, 2015, doi: 10.1109/TSTE.2014.2328298.

[19] M. Korpaas, A. T. Holen, and R. Hildrum, "Operation and sizing of energy storage for wind power plants in a market system," *Int. J. Electr. Power Energy Syst.*, vol. 25, no. 8, pp. 599–606, 2003, doi: 10.1016/S0142-0615(03)00016-4.

Metal-Containing Nanocomposites on the Basis of Isotactic Polypropylene and Butadiene-Nitrile Rubber

T.M. Guliyeva[1], N.I. Kurbanova[2], B.A. Mamedov[3], D.R. Nurullayeva[4]

Institute of Polymer Materials of the Azerbaijan National Academy of Sciences, Sumgait

Received: 22 February 2021/ Revised: 08 March 2021/ Accepted: 14 March 2021/ Published: 31-03-2021

***Abstract*—** *One and two-step methods for the synthesis of saccharin-6-carboxylic acid triglyceride were studied. The reesterification reactions of 2-hydroxypropyl-1,3-bis-ethersulfoimide of this acid and glycerol with some aliphatic saccharin-6-carboxylic acid esters were carried out. The resulting products are characterized by elemental analysis and IR spectroscopy and size exclusion chromatography. It was found that when using a two-step method, the end product is obtained with the highest yield (85%). The influence of additions of nanofillers (NF) containing nanoparticles of the copper oxide, stabilized by polymer matrix of maleinized polyethylene of high pressure (MPE), obtained by mechano-chemical method on peculiarities of structure and properties of metal-containing nanocomposites on the basis of isotactic polypropylene (PP) and butadiene-nitrile rubber (BNR) by methods of X-ray phase (RPhA) and differential-thermal analyses (DTA) and scanning electron microscopy (SEM) has been investigated. It has been revealed an improvement of the strength, deformation and rheological indices and also the thermal-oxidative stability of the obtained nanocomposites, which has been apparently connected with the synergetic effect of the interaction of the zinc-containing nanoparticles with maleic groups of MPE. It has been shown that the nanocomposites on the basis of PP/BNR/HF can be processed both by pressing method and by methods of casting under pressure and extrusion, which expands the sphere of its application.*

***Keywords*— butadiene-nitrile rubber, DTA, isotactic polypropylene, metal-containing nanocomposites, nanoparticles of zinc oxide, RPhA, SEM – analyses, thermal properties.**

I. INTRODUCTION

The modern stage of development of chemistry and technology of the composition materials is largely determined by the search for ways of creation of materials with an improved complex of properties. The intensive development of the world petrochemical industry intends a constant search for new materials possessing high consumer properties, ecological safety and simplicity of processing. Such materials are not without reason the thermoplastic elastomers (TPE). The creation of TPE is a priority direction of work in the field of polymer materials science [1, 2].

The most perspective direction of preparation of new types of TPE is the mixing of elastomers with plastics with simultaneous vulcanization of the elastomer, which leads to a high degree of dispersity of the rubber phase in the materials. TPEs obtained by this method were called thermoplastic vulcanizates (TPV). A distinctive peculiarity of TPV is the combination of the properties of vulcanized rubbers during exploitation and thermoplastics in the processing. Owing to the complex of high physical-mechanical properties, wide temperature range of working capacity, lower cost of finished products, TPVs are considered one of the most perspective classes of the polymer composite materials. Their application areas are very various [3, 4].

A large number of works on TPE and TPV has been obtained with use of polypropylene (PP) as a thermoplastics, and SKEPT, natural rubber, butadiene nitrile rubber (BNC), etc. – as elastomers. In use of various fillers or compatibilizers for improvement of the compatibility, physical-mechanical and technological properties of the compositions [5-8].

The use of solid nanoparticles (NP) of various form and chemical nature as fillers of the polymer materials opens up new possibilities of modification of the latter ones, since the surface properties of the nano-sized substance are differed by high surface energy and adsorption activity. The composition materials containing NP have a high adhesive strength of the polymer matrix with NP [9].

The creation of the metal-polymer composition materials possessing specific physical-mechanical and exploitation properties: higher heat- and electrical conductivity, high magnetic susceptibility, ability to screen ionizing radiation, etc. favored the development of investigations of nano-sized and cluster metal-containing particles in polymer matrices in many ways [10, 11].

It was known that the use of nanoparticles of d-valence metals (copper, zinc, cobalt, nickel, etc.) in polymers allows obtaining principally new materials, which are widely used in radio- and optoelectronics as magnetic, electric-conducting and optical media [9-11].

In this work, we have studied the influence of small NF additives containing NP of the metal oxides on the properties of mixture TPE based on isotactic PP and BNR.

II. EXPERIMENTAL

The following materials were used in work: isotactic PP "Kaplen" (Russia) of mark 01 030 with a molecular weight ~ 2-3×10^5, polydispersity index – 4.5, MFI – 2.3-3.6 g/10 min.

BNR – butadiene nitrile copolymer of mark NB 192 HF, containing 27% of acrylonitrile, firm BSL Olefinverbund GmbH Shckopau, d=0.98g/cm^3 (Germany).

Nanoparticles (NP) of the zinc oxide (ZnO) stabilized by polymer matrix of maleinized high-pressure polyethylene manufactured of firm Olenta (Russia), obtained by a mechano-chemical method in a polymer melt, were used as NF. A content of nanoparticles – 5 mass %, size – 26±1.0 nm, degree of crystallinity – 35 ÷ 45% [12]. A ratio of components of composition (mass %): PP/BNR/NF=50/50/(0.3; 0.5; 1.0)

The nanocomposite polymer materials have been obtained by mixing of PP with BNR and zinc-containing NF on laboratory rollers at temperature 160-165°C for 15 min. For carrying out of mechanical testing, the obtained mixtures were pressed in the form of plates with a thickness of 1 mm at 190°C and a pressure of 10 MPa.

The physical-mechanical indices of the obtained compositions were determined on the device PMI-250.

The melting flow index (MFI) was determined on the device IIRT at T=230°C, load – 5.0 kg.

The X-ray phase (RPhA) of the obtained compositions has been carried out on the device "D2 Phaser" of firm Bruker (Germany).

Thermal stability of the investigated samples of thermoelastoplasts was studied on the derivatograph of mark Q-1500D of firm MOM (Hungary). The tests were carried out in the air atmosphere in the dynamical regime at heating of the samples 5 degr·min^{-1} from 20 to 500°C, weight – 100 mg, sensitivity of the channels DTA-250mcV, TG-100, DTG-1 mV.

SEM – analysis of the obtained compositions has been carried out on the device JEOL (USA).

III. RESULTS AND DISCUSSION

The nanocomposite polymer materials on the basis of PP/BNR with zinc-containing nanofiller have been obtained. A ratio of the initial components (mass %): PP/BNR/NF = 50/50/(0.3; 0.5; 1.0).

The physical-mechanical, rheological, heat-physical and thermal properties of the obtained nanocomposites have been investigated.

In Table 1 the physical-mechanical and rheological indices of the obtained nanocomposites are presented.

TABLE 1
PHYSICAL-MECHANICAL AND RHEOLOGICAL INDICES OF THE COMPOSITION MATERIALS

Composition (mass %.), PP/BNR/NF ПП/БНК/НН	Tensile strength at break, MPa	Specific elongation, %	Vicat heat stability, °C	MFI, g/10 min
50/50/0	5.04	16	87	0.089
50/50/0.3	6.65	36	125	0.127
50/50/0.5	6.94	40	120	0.135
50/50/1.0	6.51	32	115	0.287

As is seen from data of Table 1, an introduction of 0.3 –0.5 mass % of NF into composition leads to an increase of strength index from 5.04 to 6.94 MPa. An increase of concentration of NF more than 1.5 mass % leads to the decrease of the composite strength (6.51 МПа), which has been probably stipulated by aggregation of nanoparticles leading to the formation of microdefects in a volume of the polymer matrix. An increase of NF concentration from 0.3 to 0.5 mass % leads to the decrease of deformation value at break of the composite in 2.25÷2.5 times, which has been apparently connected with the synergetic effect connected with availability of zinc-containing nanoparticles in matrix of MPE containing maleic groups, the mutual influence of which favors an increase in both deformation value and strength index. The investigation of Vicat heat stability of the obtained compositions showed that an introduction of nanofiller into composition of PP/BNR leads to the increase of heat-resistance index from 87 to 127°C in introduction of 0.5 mass % of NF, a further increase of quantity of NF leads to some decrease of heat-resistance index, which has been probably stipulated by microdeficiency of the obtained composite. At the same time, an increase of content of nanofiller (0.5-1.0 mass %) favors the increase of melting flow index (MFI) to 0.155 (0.5 mass %) and 0.287(1.0 mass %) g/10 min, which evidences about improvement of composition fluidity and possibility of its processing by casting under pressure and extrusion.

Fig. 1, 2 presents the diffractograms of RPhA of the initial PP/BNR and PP/BNR with zinc-containing nanofiller. There have been shown the reflexes corresponding to PP: d_{hkl} 6.19929; 5.17135; 4.73608; 4.48713; 4.17687; 4.03424; 3.47038; 3.11297; 2.11651 Å and a halo image is given for an amorphous BNR. On the diffractogram of the sample PP/BNR/NF (Fig. 2) there are also observed reflexes characteristic for zinc-containing NP: d_{hkl} 2.46563; 2.12992; 1.50595; 1.28812 Å, which corresponds to the series of d_{hkl} of zinc oxide – ZnO according to ASTM card file. [d-Spacings (20) – 01-071-3645 (Fixed Slit Intensity) - Cu Kα1 1,54056 A. Entry Date: 11/19/2008 Last Modification Date: 01/19/2011].

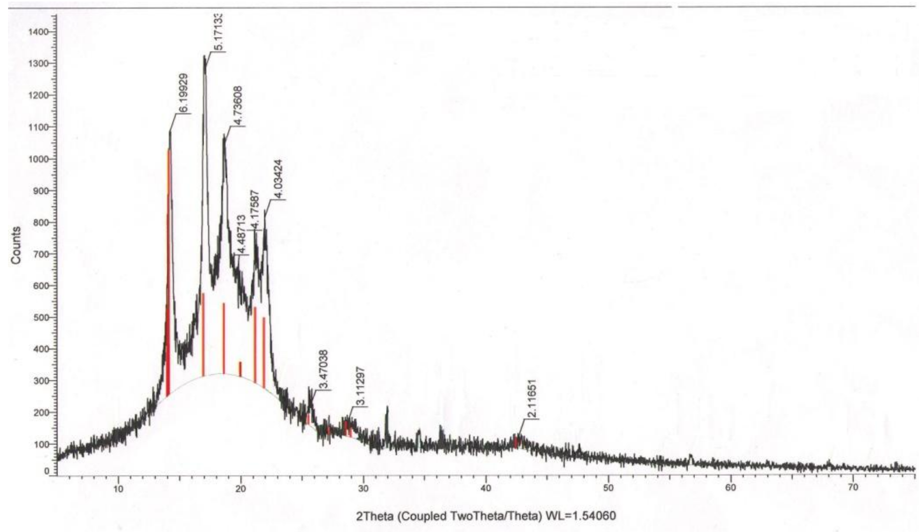

FIGURE 1: Diffractogram of PP/BNR sample

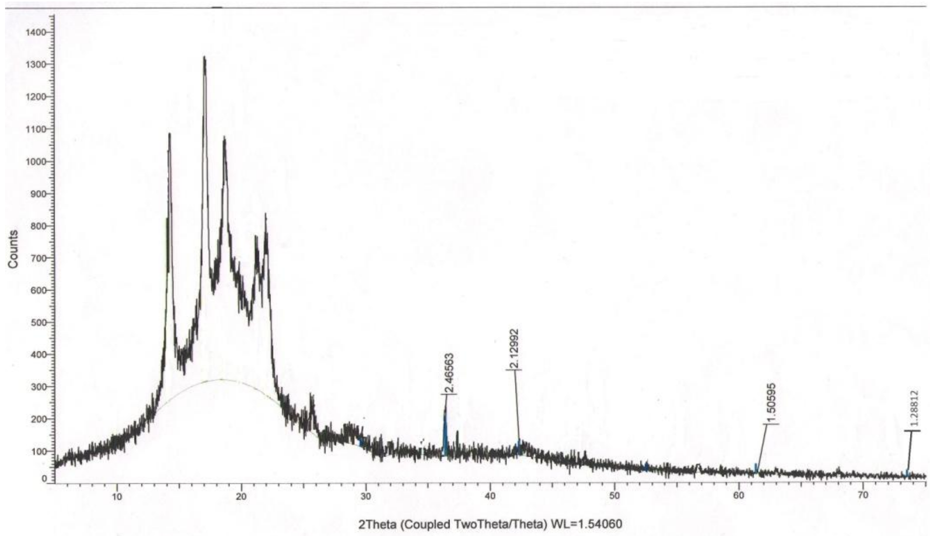

FIGURE 2: Diffractogram of PP/BNR/NF sample

Thermal stability of the investigated samples of mixed TPE on the basis of PP/BNR and PP/BNR/NF containing NF with NP of zinc oxide was estimated on activation energy (E_a) of thermal-oxidative destruction calculated by a method of double logarithm on TG curve on methodology [13], on temperature of 5% (T_5), 10% (T_{10}), 20 (T_{20}), 50% (T_{50}) decay of the investigated samples of TPE and also on their half-decay time – $\tau_{1/2}$. The data obtained as a result of derivatographic investigations are presented in Table 2.

TABLE 2
THERMAL PROPERTIES OF THE INVESTIGATED SAMPLES OF TPE

Composition (mass %.) of PP/BNR/NF	M.p., °C	T_5, °C	T_{10}, °C	T_{20}, °C	T_{50}, °C	$\tau_{1/2}$, min.	E_a, kJ·mol^{-1}
50/50/0	150	210	225	250	300	62.8	124.48
50/50/0.3	150	240	260	305	370	75.1	186.32
50/50/0.5	150	250	270	315	380	80.3	204.77
50/50/1.0	150	235	255	300	365	72.4	172.45

As can be seen from the data in Table 2, an introduction of HF containing NP of the copper oxide into the composition of mixed thermoelastoplasts favors the considerable increase of decay temperature of the samples: T_5 at 30-40°C, T_{10} at 35-45°C, T_{20} at 55-65°C, T_{50} at 70-80°C; half-decay time $\tau_{1/2,}$ is increased from 62.8 to 80.3 min., and activation energy (E_a) of decay of thermal-oxidative destruction of the obtained nanocomposites is increased by 52-80 kJ/mol, while T_m is maintained on the level 150°C. The derivatographic investigations showed that an introduction of HF containing NP of the zinc oxide into the composition of mixed thermoelastoplasts favors the improvement of thermal-oxidative stability of the obtained nanocomposites.

The numerous experimental data on mechanical, strength, relaxation and other properties of polymer-polymer and polymer-filler mixtures are explained within the framework of the concepts of the availability of interphase layer [14].

The permolecular structure of the polymer (size of spherulites, degree of crystallinity, availability of C=O groups and various branches, etc.) and the interphase interaction at the interface influences noticeably on properties of the polymer composites.

The metal-containing nanoparticles used in this work, being located at the interface of the interphase layer of the structural elements of PP, BNR and MPE favor the formation of composition of heterogeneous nucleation centers in a melt, which in the process of stepwise cooling of the nanocomposite favor the increase in crystallization centers, leading to an improvement in the crystallization process and the formation of a relatively fine-spherolite structure on the whole.

SEM analysis of the obtained composites has been carried out (Fig.3, 4).

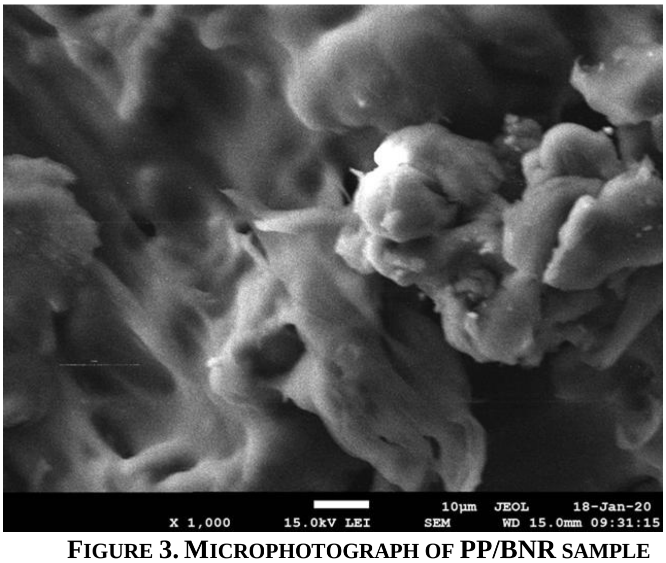

FIGURE 3. MICROPHOTOGRAPH OF PP/BNR SAMPLE

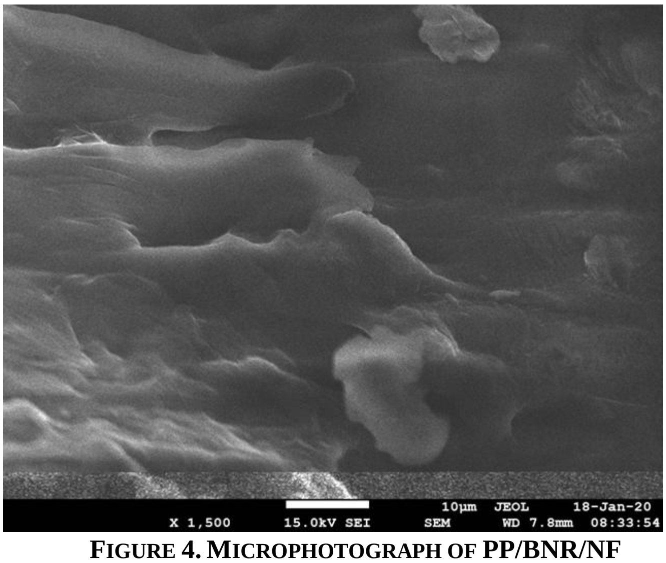

FIGURE 4. MICROPHOTOGRAPH OF PP/BNR/NF

In Fig.3, a micrography of the PP/BNR sample is presented. It is seen that the structure of the composite is quite loose with large shapeless formations. An introduction of nanofiller into the PP/BNR composition favors the formation of a fine-spherulite layered structure, which leads to an increase in the fluidity of the nanocomposite (Fig.4).

SEM-analysis of the obtained nanocomposites showed that small amounts of nanofillers (0.3 – 0.5 mass %) introduced into the polymer, obviously play the role of structure-forming agents – artificial nuclei of crystallization, which favors the appearance of a fine-spherulite layered structure in the polymer, characterized by improved physical-mechanical, rheological and thermal properties of the obtained nanocomposite [15, C.80,328].

IV. CONCLUSION

The influence of nanofiller containing nanoparticles of the zinc oxide stabilized by matrix of maleinized polyethylene (MPE), obtained by mechano-chemical method on properties of composites on the basis of PP/BNR has been investigated

The RPhA diffractograms confirm the availability of the zinc oxide nanoparticles in the composition of composites on the basis of PP/BNR.

It has been revealed the improvement of the strength, deformation and rheological indices and also the thermal-oxidative stability of the obtained nanocomposites, which has been apparently connected with the synergetic effect of the interaction of the zinc-containing nanoparticles with maleic groups of MPE.

It has been shown that the nanocomposites on the basis of PP/BNR can be processed both by pressing method and by methods of casting under pressure and extrusion.

It has been shown the prospectivity of use of the nanofiller containing zinc oxide NP, stabilized by a matrix of maleinized polyethylene, obtained by a mechano-chemical method as an additive to PP/BNR, which favors the creation of a fine-crystalline structure of the composition, in connection with which its properties are improved and thereby the areas of application of the obtained nanocomposite is expanded.

REFERENCES

[1] Polymer mixtures, vol. 2. Moscow: Mir, 1981, pp.312-338.

[2] Polymer Blends / Eds. by D. R. Paul, C. B. Bucknall. New York; Chichester; Weinheim; Brisbane; Singapure; Toronto: Wiley, 2000, 1224p.

[3] Thermoplastic Elastomers / Ed. by G. Holden, H. R. Kricheldorf, R. P. Quirk. Munich: Hanser Publishers, 2004. pp. 63-88.

[4] O. Ashpina, "TEP vs ABS," The Chemical Journal, pp. 58-61, January-February 2011.

[5] J. Karger-Kocsis, "Thermoplastic rubbers via dynamic vulcanization," in Polymer blends and alloys, G. O. Shonaike and G. P. Simon, Eds. New York: Marcel Dekker, 1999, pp. 125-140.

[6] T. I. Medintseva, E. V. Prut, and N. A. Erina, "Specifics of the structure and mechanical properties of blends of isotactic polypropylene with ethylene-propylene-diene elastomer," Polymer Science. Series A, vol. 50, pp. 647-655, June 2008.

[7] S. I. Volfson, N. A. Okhotina, A. I. Nigmatulina, R. K. Sabirov, O. A. Kuznescova, and L. Z. Achmerova, "Elastic-hysteresis properties of dynamic thermoplastics modified with nanofillers," Plast.massy, pp.42-45, April 2012.

[8] A. G. Karpov, A. E. Zaikin, and R. S. Bikmullin, "Preparation of copolymer on the basis of functionalized polypropylene and nitrile rubber in the process of their mixing," Vestn. Kaz. tekhnol. Un-ta, pp. 124-129, May 2008.

[9] Yu. A. Mikhaylin, "Polymer nanocomposition materials," Polymer materials, pp. 10-13, July 2009.

[10] A. D. Pomogaylo, A. S. Rozenberg, and I. E. Uflyand, Nanoparticles of metals in polymers. Moscow: Khimiya, 2000, 672 p.

[11] S. P. Gubin, G. Yu. Yurkov, and I. D. Kosobudsky, "Nanomaterials based on metal-containing nanoparticles in polyethylene and other carbon-chain polimers," International Journal of Materials and Product Technology, vol. 23, pp. 2-25, January-February 2005.

[12] N. I. Kurbanova, A. T. Aliyev, T. M. Guliyeva, C. K. Ragimova, C. F. Axmadbekova, N. Y. Ishenko, and D. R. Nurullayeva, "Metal-containing nanoparticles in maleinized polyethylene matrix," in PolyChar 26 World Forum on Advanced Materials. Tbilisi, 2018, p.59.

[13] Technical properties of polymer materials: Teaching-reference book / Edited by Prof. V.K.Krizhanovsky. Saint Petersburg: Profession, 2007, 240p.

[14] A. D. Pomogaylo, "Molecular polymer-polymer compositions. Synthetic aspects," Russian Chemical Reviews, vol. 71, pp. 1-31, January 2002.

[15] Encyclopedia of polymers, vol. 2. Moscow: Soviet. Encyclopedia, 1974, pp. 80, 328.

Generation of Hydrogen Gas from Crude Glycerol by Purple Non-Sulfur Photo Fermentative Bacteria, *Rhodobacter Meghalophilus*

Priya S[1], Brijesh Prasad[2]

[1]Department of Chemical Engineering, Dayananda Sagar College of Engineering, Bangalore, Karnataka, India.
[2]Department of Chemical Engineering, Ramaiah Institute of Technology, Bangalore, Karnataka, India

Received: 1 March 2021/ Revised: 9 March 2021/ Accepted: 16 March 2021/ Published: 31-03-2021

Abstract— *As the world is progressing faster with new technological innovations, the need and demand for energy is also constantly expanding. In the light of conventionally available fossil fuel reserves being exhausted extensively that has left a very deep scar on environment, the urge for alternative environment friendly energy source is the need for energy sustenance. Hydrogen gas is distinct for its high calorific value, clean fuel characteristic and suitability for wide applications. Chemical method likes steam reforming, coal gasification are established technologies available for industrial hydrogen needs but are high in terms of cost and energy input. Biological methods are promising routes for hydrogen gas generation as they can be cost effective and use a variety of organic materials as substrates. The current study is focused on generation of hydrogen gas using Rhodobacter meghalophilus, a mesophilic, and purple non sulfur photo fermentative bacteria. Crude glycerol, byproduct from biodiesel plants is used as carbon substrate because of its rich organic content. Experiments were carried out to study the effect of process parameters viz. volume of crude glycerol, pH and light intensity on generation of hydrogen gas. Crude glycerol in the media was varied from 5 – 15% (v/v), pH between 5.8 – 8.3 and the light intensity at 500, 1000 and 2000 Lx respectively. At 15% (v/v) of crude glycerol, pH of 7.8 and 1000 Lx, the volume of hydrogen gas obtained was 490 ml/L with the substrate to hydrogen gas conversion rate as 0.012 mol/ mol of crude glycerol with light conversion efficiency of 1.16%.*

***Keywords—* Bio hydrogen, Clean energy, Crude glycerol, Photo fermentation, Rhodobacter meghalophilus.**

I. INTRODUCTION

The world is progressing ahead with tremendous improvement in technology and is also facing challenges on energy survival. The world had largely relied on the use of fossil fuels to meet its energy needs. The energy needs have been increasing enormously with advancements in industrial, transport, agricultural sectors, causing rapid depletion of fossil fuels that have been the prime fuel reserve. The liberal use of fossil fuels has also left a serious impact on the ecosystem. The burning of fossil fuels has released exorbitant amount of carbon di oxide that is changing the ecological and geological characteristics of our planet. With the depleting fossil fuel sources, ever rising demand for energy and the hazardous damages caused by fossil fuels, the world's energy requirements rely largely on the search for other alternative resources.

The potential of solar, wind, ocean, geothermal and hydrogen energies are being tapped in for bridging the energy gap. The advantage of these alternative sources is that they are also renewable and environment friendly. Vast amount of research has been carried out to study the potential methods to optimize the energy derivation form these renewable sources. Of these, studies on hydrogen gas as an alternate energy source has gained more momentum due to their advantages that it has high energy content and is eco-friendly, producing only water as it's by product on burning (1). These advantages have proved to show that hydrogen fuel can be seen as a positive substitute to reduce our dependency on fossil fuels.

II. LITERATURE

Unlike solar, wind energy, hydrogen is not freely found in nature. Hydrogen is being used as a raw material in manufacturing plants producing ammonia, plastics, petrochemicals and also in refineries (2), which is commercially produced by chemical methods such as steam methane reforming, coal gasification [3], partial oxidation of hydrocarbons [4] etc. These methods have proven technology but are also energy intensive. Therefore, biological methods are being researched upon to study the production of hydrogen gas by processes such as direct photolysis, indirect photolysis, dark fermentation, photo fermentation, anaerobic fermentation and hybrid fermentation [4] employing microorganisms belonging to the family of green algae [5], cyanobacteria [6], photosynthetic bacteria [7], fermentative bacteria [8]. The use of biological methods will help to generate the hydrogen gas with minimum requirements.

2.1 Microbial substrates for bio hydrogen generation process

Microorganisms depend on carbon as the main source of substrate for hydrogen generation. Simple sugars like glucose, sucrose or lactose are used for bio hydrogen gas generation [9]. However, the use of these sugars as pure source of carbon may not be feasible as the cost of substrate becomes one of the limiting factors while scaling the process. Therefore, to make the process economically viable, cheaper sources of carbon needs to be found as alternative substrates. Runoffs from agriculture [10], dairy [11] and food processing industries [12], brewery industries [13] and municipal solid waste [14] are rich source of carbohydrates such as starch or cellulose. Currently these materials are productively used for biogas generation or simply dumped on landfills and into water bodies. Land or water disposal of these materials are posing severe environmental threats and endangering several life forms in the ecosystem. Therefore, efforts are being made to amalgamate these organic wastes as carbon substrates for hydrogen production through microbial conversion process [15].

2.1.1 Crude Glycerol as a source of carbon substrate for bacteria to generate hydrogen gas

Biodiesel is one of the alternative energy sources that have been a promising substitute for fossil fuels. As such, the number of biodiesel plants is increasing worldwide and the production of biodiesel is also scaled up gradually. In the process of biodiesel production, a byproduct that is equivalent to about 10% (by mass) of biodiesel, known as crude glycerol is produced [16]. Unreacted free fatty acids from vegetable oil and chemicals used in the production of biodiesel such as methanol, sulphuric acid, sodium hydroxide and soap, formed during trans-esterification reaction, find their way along with this glycerol [17]. It is therefore termed crude, for it is highly impure and cannot be used in pharmaceutical, food or cosmetic industries that otherwise use glycerol as one of the raw materials.

Crude glycerol can be chemically treated to remove the impurities and converted to value added products. The conventional treatment steps include a series of unit operations or processes like acidification, neutralization, extraction, adsorption and filtration [18]. But the cost of the treatment processes makes it an unviable option. Therefore, crude glycerol from biodiesel plants are considered as waste material and dumped off. This method of disposal is also hazardous to the environment due to the presence of methanol, sulphuric acid and sodium hydroxide. Therefore, ways to efficiently treat crude glycerol or use them as raw materials to generate value added products can be economically beneficial to the biodiesel industries and also prevent hazard to environment due to their direct disposal.

As chemical treatment of crude glycerol is not cost effective, biological ways of its treatment can be explored as a possible and eco-friendly option due to the rich organic content. Microbial degradation of crude glycerol by fermentation process is an alternative and promising way of treating crude glycerol for its effective usage [19].

Many bacterial species in the mesophilic and thermophilic family, have been studied for their ability to decompose crude glycerol and generate value added products such as lactic acid, propane diol etc [20]. In this regard, microorganisms capable of synthesizing hydrogenase and nitrogenase enzymes have been found to generate hydrogen gas as a metabolic product through bioconversion process via photosynthesis or fermentation [21]. Bacterial species such as *E.coli* [22], purple non sulfur bacteria such as *Rhodobacter sphaeroids* [23], *Rhodobacter palustris* [24], *Enterobacter* [25], *Clostridium* [26] *etc* have the potential to generate hydrogen gas utilizing the rich carbon source available in the crude glycerol.

2.2 Hydrogen generation by photo fermentation

Photo fermentation deals with conversion of organic substrate in the presence of light to produce biomass or metabolic products that have various end uses. A diverse group of photosynthetic bacteria act on the organic substrates under anaerobic condition to generate bio hydrogen by the enzymatic activity of hydrogenase and nitrogenase [27]. The overall reaction of hydrogen production by photo fermentation is according to the reaction (1):

$$C_6H_{12}O_6 + 6H_2O + h_v \rightarrow 12H_2 + 6CO_2 \quad (1)$$

All plants, algae and some bacteria are capable of photosynthesis utilizing, light as the source of metabolic energy. *Cyanobacteria* have been frequently studied for its potential to generate hydrogen by oxygenic photosynthesis [(28)]. However, the purple non sulfur bacteria such as *Rhodobacter* have much higher potential for hydrogen generation by both oxygenic photosynthesis and photo fermentation [(29)].

III. METHODOLOGY

The chemicals used for the experimental study were of analytical grade. The strain $JA194^T$ was obtained from JNTU, Hyderabad. Crude glycerol was sourced from Biofuel Park, GKVK, Bangalore. The media for strain $JA194^T$ was prepared using crude glycerol, yeast extract (0.3 g/L), C_2H_3O (0.5 ml/L), $C_4H_4Na_2O_4$ (1 g/L), $C_2H_7NO_2$ (0. 5g/L), 0.1% of $C_6H_5FeO_7$ solution (5 ml/L), KH_2PO_4 (0.5 g/L), $MgSO_4.7H_2O$ (0.4 g/L), NaCl (0.4 g/L), NH_4Cl (0.4 g/L), $CaCl_2.2H_2O$ (0.05 g/L), vitamin B_{12} solution (0.4 ml/L), trace element solution (1 ml/L). The composition of trace element solution consisted of $ZnSO_4.7H_2O$ (0.1 g/L), $MnCl_2.4H_2O$ (0.03 g/L), H_3BO_3 (0.3 g/L), $CoCl_2.6H_2O$ (0.2 g/L), $CuCl_2.6H_2O$ (0.01 g/L), $NiCl_2.6H_2O$ (0.02 g/L), $Na_2MoO_4.2H_2O$ (0.03 g/L).

Crude glycerol contains unreacted free fatty acids, chemicals such as methanol, sulphuric acid used in transesterification of vegetable oil during biodiesel production process, soap, glycerol and water. The amount of glycerol present in the sample was determined by titrimetric method based on cold oxidation of crude glycerol in a strong acidic medium as given by the equation (2):

$$CH_2OH\text{-}CHOH\text{-}CH_2OH + 2NaIO_4 \rightarrow HCOOH + 2HCOH + 2NaIO_3 + H_2O \quad (2)$$

The mixture was then titrated against a base and glycerol content in the sample (m/m) was calculated by the formula:

$$((V_1 - V_2) \times T \times 0.0921 \times 100)/\ m \quad (3)$$

where V_1 and V_2 are the volume of sodium hydroxide used for titration of the reacted sample and the blank respectively. T is the normality of sodium hydroxide used in titration and m is the mass of crude glycerol sample.

The experimental studies on fermentation process for generation of hydrogen gas was carried using a 0.5L, 4 neck jacketed glass reactor. One neck was used for introducing the inoculum and to flush nitrogen into the reactor to maintain anaerobic condition. A K-type thermocouple was inserted through the second neck to monitor the temperature in the reactor. A light source was introduced in to the reactor through its third neck to facilitate the supply of light as *Rhodobacter meghalophilus* is a photo fermentative bacterium. A tube was inserted in the fourth neck of the reactor and the other end of the tube was inserted into an inverted cylinder arrangement to collect the hydrogen gas by water displacement method.

300 ml of the sterilized growth media was used for inoculation in batch fermentative tests. In order to maintain anaerobic condition, nitrogen was flushed in the reactor. 0.25% of L-Cysteine, an amino acid that acts as a reducing agent was also added to maintain anaerobic condition. The parameters such as volume percentage of crude glycerol in the media, pH and the intensity of light source were studied for their effect on *R. meghalophilus* for hydrogen gas production. The gas generated was monitored by the volume of water displaced in the inverted cylinder in a water trough. The percentage of hydrogen in the gas sample was analyzed by GC with TCD and also by a hydrogen gas sensor.

IV. RESULTS AND DISCUSSION

The amount of glycerol present in sample of crude glycerol was determined to be 26% (m/m) by titrimetric test. The amount of crude glycerol added to the nutrient media was varied between 5 to 15% (v/v). As the pH range for bacterial growth is optimum near to neutral range, experimental trials were carried out at pH 5.8, 6.8, 7.8 and 8.3. Effect of light intensity was studied at 500, 1000 and 2000 lx respectively.

4.1 Effect of crude glycerol on biohydrogen production

The amount of crude glycerol, added as carbon substrate in the nutrient media was varied between 5 to 15% (v/v) to study its impact on the growth of bacteria and hydrogen gas generation. The volume of gas collected during the growth period of bacteria in the fermentation process was recorded as shown in the fig. 1.

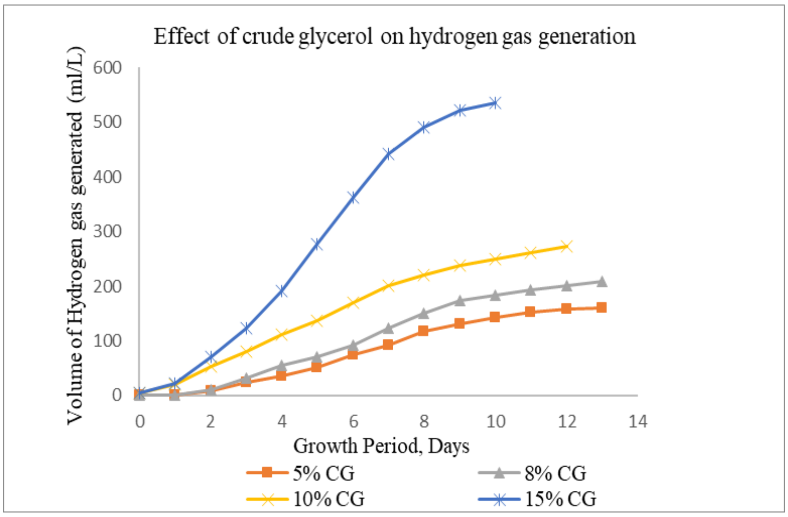

FIGURE 1: Effect of crude glycerol on hydrogen gas generation

It was observed that the growth of bacteria was influenced by the glycerol concentration in the medium. The bacterial growth was influenced by the length of the lag phase that varied with glycerol concentration. It can be seen that the lag phase in the growth of bacteria was more when crude glycerol in the nutrient medium was added in 5% and 8% (v/v) respectively. As the volume of crude glycerol in the nutrient medium increased gradually to 10% and 15% (v/v) respectively, the lag phase was found to be shortened. This shows that enzymatic activity of nitrogenase increases with increase in the volume of crude glycerol in the medium. Thus, increasing the volume of crude glycerol in nutrient medium is beneficial for hydrogen production. But, the soap content in its composition also increases. The effect of increase in soap content in the medium was noticed with foam formation when the crude glycerol was increased above 15% (v/v) in the nutrient medium. Therefore, batch experimental studies were carried out with crude glycerol volume varied between 5 -15% (v/v). The study showed that the volume of hydrogen gas generated was high when 15% (v/v) of crude glycerol was added to the growth medium. In the experimental trials, 490 ml/L of gas was found to be generated with 15% (v/v) of crude glycerol in the medium.

4.2 Effect of pH

Bacteria are sensitive to changes in pH due to which their metabolic pathways are altered that in turn affect the substrate degradation. The pH of the standard growth medium was found to be 6.4. With addition of crude glycerol, the pH of the medium was 6.9 due to alkaline nature of crude glycerol that contains soaps, formed by reaction of free fatty acids with alkali in transesterification reaction in biodiesel production. The pH of the growth medium in batch fermentative trials was varied between 5.8 to 8.3 and the volume of hydrogen gas generated was observed. Fig.2 shows the volume of hydrogen gas collected with pH of the medium at 5.8, 6.8, 7.8 and 8.3 respectively.

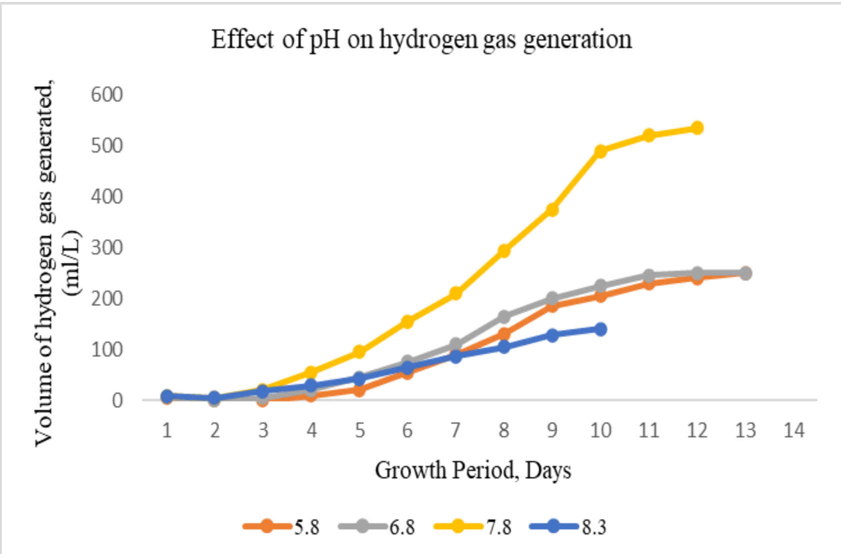

FIGURE 2: Effect of pH on hydrogen gas generation

As pH of the growth medium increased to slightly alkaline, gradual reduction in lag phase was noticed which was reflected by the difference in the volume of gas collected for fermentation trials at different pH values? The volume of hydrogen gas was found to increase with pH of the medium at 5.8, 6.8 and 7.8, but showed a decrease in volume for pH 8.3. The volume of gas produced was observed to be high at 490 ml/L for tests carried out when pH of the medium was increased to 7.8. At 8.3 pH, the volume of gas generation was found to decrease compared to lower pH values. As hydrogen gas is produced as a metabolic product in anaerobic fermentation, the decrease in gas production shows that the substrate degradation by the bacteria started to decrease at pH of 8.3. This could be due to changes in cellular activities of the microorganism.

4.3 Effect of light intensity

R.meghalophilus is a photo fermentative bacteria. In addition to the carbon source in the nutrient medium, the bacteria also derive its energy for growth from light. Hydrogen production rate has been found to exhibit a linear relation with intensity of light. Therefore, the effect of light intensity on hydrogen production was studied at 500, 1000 and 2000 lx in the photo fermentative tests. Fig. 3 shows the effect of light intensity on hydrogen gas generation by photo fermentation.

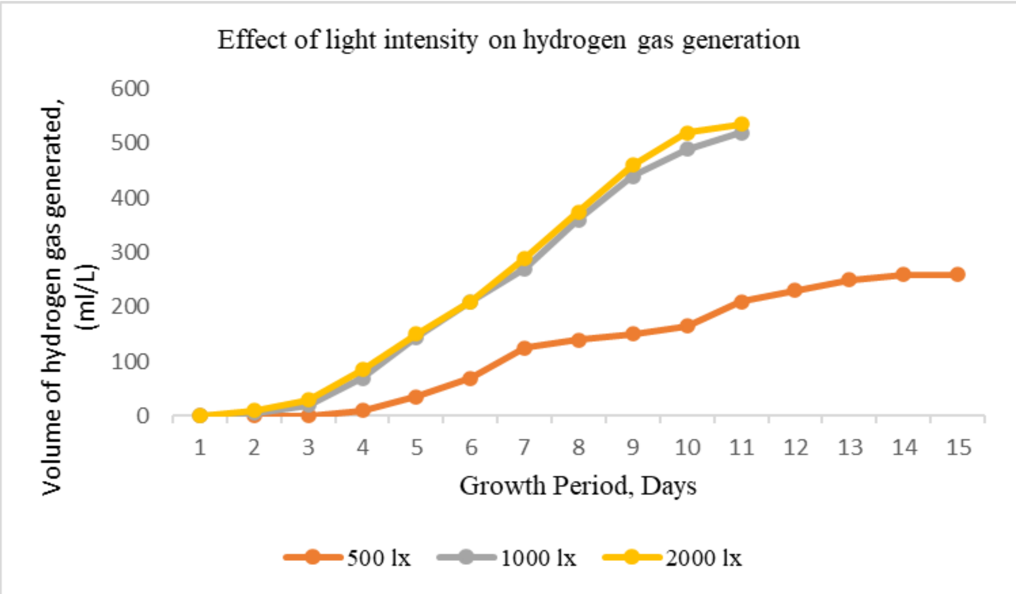

FIGURE 3: Effect of light intensity on hydrogen gas generation

With increase in the light intensity, the lag phase in the bacterial growth was observed to be shorter than lower light intensity. The volume of hydrogen gas increased with increase in light intensity from 500 to 2000 lx. However, the volume of hydrogen gas at 2000 lx was close in range with that obtained at 1000 lx. Light conversion efficiency is significant in photo fermentation and is estimated by comparing the thermal combustion value of hydrogen gas generated with absorption of light intensity as calculated by the formula (4):

$$\varepsilon = [(33.61 \cdot \rho \cdot V_{H2})/(I \cdot A \cdot t)] \cdot 100 \quad (4)$$

Where V_{H2} is the volume of hydrogen generated in L, ρ is the density of the hydrogen gas in g/L, I is the light intensity in W/m^2, A is the irradiated area in m^2 and t, time for hydrogen gas generation.

The Efficiency of light conversion has been found to be 0.55%, 1.16% and 1.13% for 500 lx, 1000 lx and 2000 lx respectively. Therefore, light intensity of 1000 lx is taken as the light saturation point at which a maximum of 490 ml/L of hydrogen gas was collected with light conversion efficiency of 1.16%.

4.4 Hydrogen gas yield

The volume of hydrogen gas collected during the batch fermentation tests was analyzed by a hydrogen gas sensor to determine the concentration of hydrogen in the gas. The sensor was made of SnO_2 whose thermal conductivity varies with the concentration of hydrogen gas. The concentration of hydrogen in the gas sample was found to be 457 mg/L with glycerol concentration of 15% (v/v), pH at 7.8 and light intensity of 1000 lx. The yield of hydrogen gas was calculated to be 0.012 mol/ mol of crude glycerol.

V. CONCLUSIONS

Hydrogen gas can be a promising alternative source of energy that can drive the future world. While the industrial demand for hydrogen gas is currently met by energy intensive, chemical methods of production, they are unsustainable in terms of production cost and environmental pollution. Biological methods can be promising as they do not demand energy and can employ wide family of bacterial species that can act on various organic waste materials to generate hydrogen gas. This is seen as a promising way to meet the future energy demand. In the present study, *Rhodobacter meghalophilus* from the family of *Rhodobacter* was identified and investigated for its capability to generate hydrogen gas. As crude glycerol is used as carbon substrate for the bacterium in the fermentation process, its effect on hydrogen gas generation was studied by varying the volume of crude glycerol in the nutrient medium in 5, 8, 10 and 15% (v/v). pH and light intensity are two other significant parameters that impacts the bacterial growth and the hydrogen gas generation in photo fermentation process. pH of the medium was varied between 5.8 to 8.3 and the light intensity of 500, 1000 and 2000 lx was used in photo fermentation runs.

From the experimental runs carried out with the above study parameters, 490 ml/L of gas was collected with the hydrogen concentration of 457 mg/L by using 15% (v/v) of crude glycerol in the nutrient medium, pH of 7.8 and light intensity of 1000 lx. As the bacteria are photo fermentative, the process needs the presence of light along with a carbon substrate for its energy supplementation and hydrogen gas generation. Thus, to make the process further sustainable, solar cells could be used to power the light source for the photo fermentation process.

ACKNOWLEDGEMENT

We thank the management of Dayananda Sagar College of Engineering and Ramaiah Institute of Technology for their support and encouragement, Prof. Sasikala, Jawaharlal Nehru Technological University and Mr. Rajesh, Biofuel park, Gandhi Krishi Vignyan Kendra, for their help and guidance.

REFERENCES

[1] N.P Brandon, Z. Kurban,"Clean energy and the hydrogen economy," Philosophical Transactions of Royal Society, London, vol. A 375: 20160400, 2017. http://dx.doi.org/10.1098/rsta.2016.0400.

[2] F. Ausfelder, A. Bazzanella, "Hydrogen in the Chemical Industry" Hydrogen Science and Engineering: Materials, Processes, Systems and Technology, pp. 19 – 40, 2016. https://doi.org/10.1002/9783527674268.ch02.

[3] Ahmed Aidid Ibrahim., "Hydrogen Production from Light Hydrocarbons," Advances in Hydrogen Generation Technologies, 2018.

[4] G. Mahidhara, H. Burrow, C. Sasikala, et al. "Biological hydrogen production: molecular and electrolytic perspectives," World Journal of Microbiology and Biotechnology, vol.35, 116, 2019. https://doi.org/10.1007/s11274-019-2692-z.

[5] J.Wang, Y. Yin, "Fermentative hydrogen production using pre-treated microalgal biomass as feedstock," Microbial Cell Factories . vol.17, 22, 2018. https://doi.org/10.1186/s12934-018-0871-5.

[6] K. Kolbe, S. Lechtenböhmer, M. Fischedick, "Hydrogen derived from algae and cyanobacteria as a decentralized fueling option for hydrogen powered cars: Size, space, and cost characteristics of potential bioreactors," International Journal of Sustainable Transportation, pp. 1–10, 2019. doi:10.1080/15568318.2018.1547935.

[7] I. Suleyman, Allakhverdiev et al., "Photosynthetic hydrogen production, Journal of Photochemistry and Photobiology C: Photochemistry Reviews," vol.11, pp. 101-113, 2010. ISSN 1389-5567, https://doi.org/10.1016/j.jphotochemrev.2010.07.002.

[8] C. Ding, K Yang, K, & J. He, "Biological and fermentative production of hydrogen," Handbook of Biofuels Production, *303–333*, 201, 2016. doi:10.1016/b978-0-08-100455-5.00011-4.

[9] S Eker, & M. Sarp, "Hydrogen gas production from waste paper by dark fermentation: Effects of initial substrate and biomass concentrations," International Journal of Hydrogen Energy, vol. 42(4), pp. 2562–2568, 2017. doi:10.1016/j.ijhydene.2016.04.020

[10] A. Tawfik, A H Salem, "Optimization of hydrogen production from pretreated rice straw waste in a mesophilic up-flow anaerobic staged reactor," International Journal of Energy Research, vol.38, pp. 1155 – 1161, 2014.

[11] M. Krishnaveni, "Bio-Hydrogen Production from the Dairy Waste Water using Anaerobic Sequence Batch Reactor," International Journal for Scientific Research & Developmen, vol.6 (4), 2018. ISSN (online): 2321-0613.

[12] Giovanna Cappai., et al. "Biohydrogen Production from Food Waste: Influence of the Inoculum-To-Substrate Ratio," Sustainability, vol. 10, pp. 4506, 2018. doi:10.3390/su10124506.

[13] S. Vijaya Krishna, et al., "Biohydrogen production from brewery effluent in a batch and continuous reactor with anaerobic mixed microbial consortia," Biofuels. Vol. 8(6), pp. 701–707, 2016. doi:10.1080/17597269.2016.1206409.

[14] M.M Yeshanew, et al., "Co-production of Hydrogen and Methane from the Organic Fraction of Municipal Solid Waste in a Pilot Scale Dark Fermenter and Methanogenic Biofilm Reactor," Frontiers in Environmental Science, vol. 6:41, 2018. doi:10.3389/fenvs.2018.00041.

[15] D. Das, "A Road Map on Biohydrogen Production from Organic Wastes. Transactions of the Indian National Academy of Engineering," vol.2, pp. 153–160, 2017. https://doi.org/10.1007/s41403-017-0031-y.

[16] Rahul Mangayil, Matti Karp, Ville Santala., "Bioconversion of crude glycerol from biodiesel production to hydrogen," International Journal of Hydrogen Energy, vol.37 (17), pp. 12198-12204, 2012. ISSN 0360-3199. https://doi.org/10.1016/j.ijhydene.2012.06.010.

[17] Shengjun Hu, Xiaolan Luo, Caixia Wan, Yebo Li, "Characterization of Crude Glycerol from Biodiesel Plants," Journal of Agricultural and Food Chemistry, vol. *60* (23), pp. 5915-5921, 2017. doi: 10.1021/jf3008629.

[18] X. Yang, X. Guomin, V. Arvind, "A universal procedure for crude glycerol purification from different feedstocks in biodiesel production: experimental and simulation study," Industrial and Industrial Chemistry Research, vol. 52 (39), pp. 14291-14296, 2013. https://doi.org/10.1021/ie402003u.

[19] Wang Xiao-Li, Zhou Jin-Jie. Sun Ya-Qin. Xiu Zhi-Long, "Bioconversion of Raw Glycerol from Waste Cooking-Oil-Based Biodiesel Production to 1,3-Propanediol and Lactate by a Microbial Consortium," Frontiers in Bioengineering and Biotechnology 7:14, 2019. Doi:10.3389/fbioe.2019.00014.

[20] L. Mitrea, M. Trif, A.F Cătoi, *et al*, "Utilization of biodiesel derived-glycerol for 1,3-PD and citric acid production," Microbial Cell Factories, vol. 16, pp. 190, 2017. https://doi.org/10.1186/s12934-017-0807-5.

[21] Dipankar Ghosh, Patrick C Hallenbeck, "Cyanobacteria and photosynthetic bacteria: metabolic engineering of hydrogen production," Advances in enzymatic conversion of Biomass to biofuels, 1st Edition, Future Science Groups, UK. http://www.future-science.com.

[22] Toshinari Maeda, et al, "Current state and perspectives in hydrogen production by Escherichia coli: roles of hydrogenases in glucose or glycerol metabolism," Applied Microbiology and Biotechnology, vol. 102, pp.2041 – 2050, 2017. https://doi.org/10.1007/s00253-018-8752-8.

[23] A. Thitirut Assawamongkholsiri, Alissara Reungsang, "Photo-fermentational hydrogen production of Rhodobacter sp. KKU-PS1 isolated from an UASB reactor," Electronic Journal of Biotechnology, vol.18, pp. 221–230, 2015.

[24] D. Zhang, et al, "Bioprocess Modelling of Biohydrogen Production by Rhodopseudomonas palustris: Model Development and Effects of Operating Conditions on Hydrogen Yield and Glycerol Conversion Efficiency," Chemical Engineering Science, vol. 130, pp. 68-78, 2015.

[25] Y. Li, Y. Qiu, X. Zhang, *et al*, "Strain screening and optimization of biohydrogen production by *Enterobacter aerogenes* EB-06 from glycerol fermentation," Bioresources and Bioprocessing vol. 6, pp. 15, 2019. https://doi.org/10.1186/s40643-019-0250-z.

[26] M.A Jáuregui, A. Ladino, & D. Malagón-Romero, "The effect of the initial concentration of glycerol on the hydrogen produced by strains of the genus Clostridium spp. International Journal of Sustainable Engineering," vol. 11(3), pp. 205–210. doi:10.1080/19397038.2017.1387826.

[27] S. Priya, B. Brijesh, K.R Reddy, C.V Reddy, N.P Shetti, R.V Kulkarni, & A.V Raghu, "Prospects of Biohydrogen Production from Organic Waste - A Review," *Chemical Engineering & Technology, 2020.* doi:10.1002/ceat.201900400 .

[28] Ghiasian M, "Biophotolysis - Based Hydrogen Production by Cyanobacteria. In: Prospects of Renewable Bioprocessing in Future Energy Systems. Biofuel and Biorefinery Technologies," vol 10. https://doi.org/10.1007/978-3-030-14463-0_5.

[29] D. Akroum-Amrouche, H. Akroum, H. Lounici, "Green hydrogen production by Rhodobacter sphaeroides. Energy Sources, Part A: Recovery," Utilization, and Environmental Effects, pp1–19, 2019. doi:10.1080/15567036.2019.1666190.

AD Publications

Sector-3, MP Nagar, Bikaner,

Rajasthan, India

www.adpublications.org, info@adpublications.org